



On the effective resolution of TMS, its tradeoff with signal-to-noise ratio, and the experimental implications

Tuomas P. Mutanen^a, Victor H. Souza^a, Jaakko O. Nieminen^a and Risto J. Ilmoniemi^a

^a*Department of Neuroscience and Biomedical Engineering, Aalto University,
P.O. Box 12200, 00076 AALTO, Espoo, Finland*

Correspondence: Tuomas Mutanen, ^a*Department of Neuroscience and Biomedical Engineering, Aalto University,
P.O. Box 12200, 00076 AALTO, Espoo, Finland*

Email: tuomas.mutanen@aalto.fi Website: www.tuomas.mutanen.com/science Phone: +358 3256270

Abstract. Experimental data have indicated that transcranial magnetic stimulation (TMS) has high spatial specificity. For instance, even a millimeter-scale movement of the TMS coil above the motor cortex can change the recorded response in peripheral muscles drastically. However, such a small coil displacement induces a cortical electric field that overlaps considerably with the original electric field. Here, we describe how the basic electrophysiological properties of neurons can explain the apparent high spatial resolution of TMS. We show with simulations that a TMS intensity close to the neuronal threshold yields the highest spatial resolution, albeit with a possible tradeoff with the signal-to-noise ratio. The simulations suggest that with such a TMS intensity, the activated cortical area is significantly smaller than the area in which the electric field exceeds its half-maximum strength.

Keywords: transcranial magnetic stimulation, focality, resolution, electrophysiology, modelling

1. Introduction

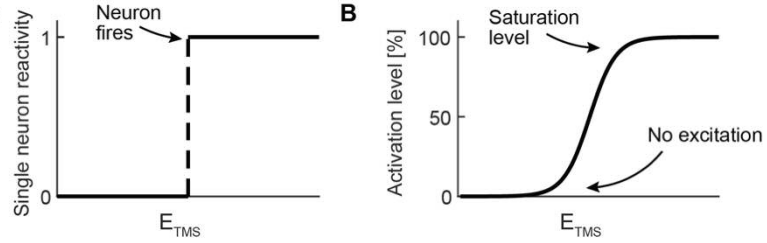
Experimental evidence from the mapping of the motor areas suggests that transcranial magnetic stimulation (TMS) can activate the cortex with high focality, producing specificity comparable to invasive methods (Picht et al., 2011). However, electric field (E-field) computations, performed in simplified spherical (Ravazzani et al., 1996) or anatomically realistic geometries (Thielscher et al., 2015), as well as direct measurements (Nieminen et al., 2015) have shown that the TMS-induced E-field is, in fact, relatively smeared. For a modern figure-of-eight coil, the area in which the E-field exceeds its half-maximum strength is approximately 40 mm wide and 80 mm long (Nieminen et al., 2015). Superficially, there seems to be a discrepancy between the spread of the TMS-induced E-field and the effective focality of brain activation; e.g., for the abductor pollicis brevis (APB) muscle, at 110% of the resting-motor-threshold intensity, an effective stimulation region of only ~15 mm wide has been measured (Koponen et al., 2018). Here, we describe how the basic physiological properties of neurons lead to a non-linear response behaviour that can explain the high effective resolution of TMS. We tested our hypothesis in an open-source realistic multi-scale brain-stimulation model (Aberra et al., 2020). We list some testable predictions this electrophysiological hypothesis makes and go through some implications for experimental work. Recently, relatively high stimulus intensities have been promoted for improving the signal-to-noise ratio (SNR) of genuine cortical

TMS-evoked electroencephalography (EEG) potentials (TEPs) (Belardinelli et al., 2019). We comment on this approach in light of the simulation results.

2. Theory

TMS induces in the cortex a strong E-field (\mathbf{E}_{TMS}), which depends on the geometry and placement of the stimulation coil, the stimulus intensity, and the conductivity profile of the head. If the E-field strength at a neuron is sufficient, the cell fires an action potential. The activation curve of a single neuron is a step function (Fig. 1 A), whose threshold depends on the E-field waveform, as well as the fine geometrical and electrophysiological properties, the excitability state¹, and the orientation of the cell w.r.t. \mathbf{E}_{TMS} (Aberra et al., 2020). Because there is variability in the neuron-specific E-field thresholds, the net activation of a small cortical patch exhibits an S-like behaviour as a function of the E-field strength (Fig. 1 B). If the TMS intensity is close to the excitation thresholds, only very few neurons are activated at the tails of \mathbf{E}_{TMS} . On the other hand, when operating above the saturation level, the number of activated neurons decreases first very slowly when moving away from the maximum location of \mathbf{E}_{TMS} , resulting in low effective focality.

Figure 1. The reactivity of neurons as a function of E_{TMS} . **A)** The response function of a single cell to TMS is a step function; the cell either stays inactive (0) or launches an action potential (1). **B)** A focal cell population consists of individual neurons with slightly different excitation thresholds to TMS. Thus, the response curve of the whole cell population is a smooth sigmoidal curve.



3. Methods

Using SIMNIBS software, we modelled \mathbf{E}_{TMS} in realistic and spherical geometries (Thielscher et al., 2015). A spherical head was included to visualize the E-field and neuronal activation without the distortions due to the cortical folding to highlight the direct effects of the non-linear responsiveness of neurons. In the realistic and spherical geometries, the cortical surfaces were represented by 277,742 and 20,738 triangle elements, respectively. The modelled TMS coil was the Magstim 70-mm figure-of-eight coil (P/N 9790). The neuronal excitations due to \mathbf{E}_{TMS} were modelled in layer-5 pyramidal cells (Aberra et al., 2020). In the realistic cortex mesh, each triangle element contained 500 neurons of five different morphologies derived from the Blue Brain Project (Ramaswamy et al., 2015). The main axes of the dendritic trees were set perpendicular to the triangle, and each of the 100 copies of a single cell morphology was rotated evenly around the triangle-element normal. \mathbf{E}_{TMS} was assumed to be uniform across the whole cell, and the cellular activation due to \mathbf{E}_{TMS} was modelled using the extracellular potential mechanism implemented in NEURON (Hines and Carnevale, 2003; Aberra et al., 2020). In the 80-mm-radius spherical cortex, each triangle contained 6,500 neurons (from five different morphologies) pointing to all possible directions with even distribution.

In the realistic model, the coil was placed on the scalp with its centre over the hand knob of the left primary motor cortex, and the orientation was set approximately

¹ The balance of inhibitory and facilitatory post-synaptic current affecting upon the soma.

perpendicular to the central sulcus. The coil was modelled to move in ~ 3 -mm steps along the scalp from -30 to 30 mm relative to the original spot, along the axis of the wings of the modelled figure-of-eight coil. In the spherical model, the coil was placed tangential to the 95 -mm-radius scalp surface. The TMS pulse was monophasic (100 - μ s-long half cycle) with maximum dI/dt ranging from 0 to 300 MA/s (producing maximum E_{TMS} strengths of 0 – 400 V/m).

In the realistic cortex, the mean focality for each stimulation intensity, across all coil locations, was estimated both in terms of E_{TMS} and the neuronal activation level. The focality was defined as the cortical area showing 50% or more of the maximum E_{TMS} strength/activation level. In the spherical cortex, E_{TMS} and the activation level were computed along the axis of the coil wings.

4. Results

The simulations supported the hypothesis; at intensities below ~ 200 MA/s, the effective focality was better than the focality of the E-field (Fig. 2 A). Above ~ 230 MA/s, however, the saturation of the cortical populations led to poorer focality than suggested by the shape of E_{TMS} . The same was true in the spherical cortical model (Fig. 2 B); comparatively low stimulation intensity (200 MA/s) led to a narrower activation profile compared to the E-field profile, whereas at 300 MA/s, the activation profile in the region where the E-field exceeded its half-maximum value, almost matched the E-field profile. This improved focality at a low TMS intensity came, however, at the expense of reduced overall activation level. Representative E-field-strength and activation distributions in the realistic cortex are shown in Fig. 3.

Figure 2. Focality as a function of the TMS intensity. **A)** Realistic cortical model: The focality was measured as the percentage of the cortical area showing 50% or more of the maximum E-field strength or activation level. The E_{TMS} focality (solid line) stays constant, but the mean area of the cortical activation (dotted line) increases with the intensity. The gray shaded area shows standard deviation across coil locations. **B)** Spherical cortical model: The solid line corresponds to the E-field (the left y-axis) profile, and dashed and dotted lines correspond to the activation (the right y-axis) profiles at 200 and 300 MA/s, respectively, along the axis of the coil wings.

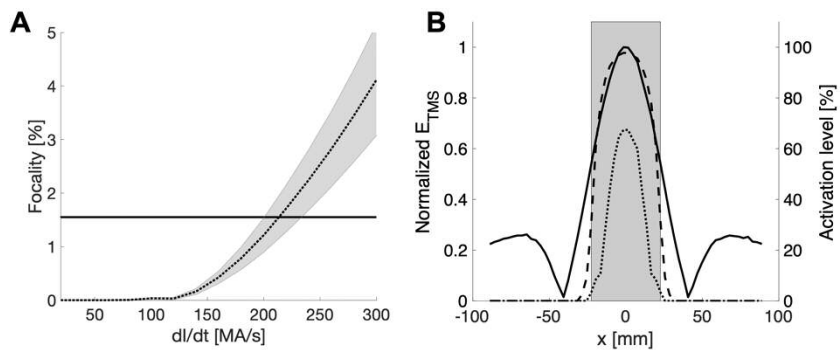
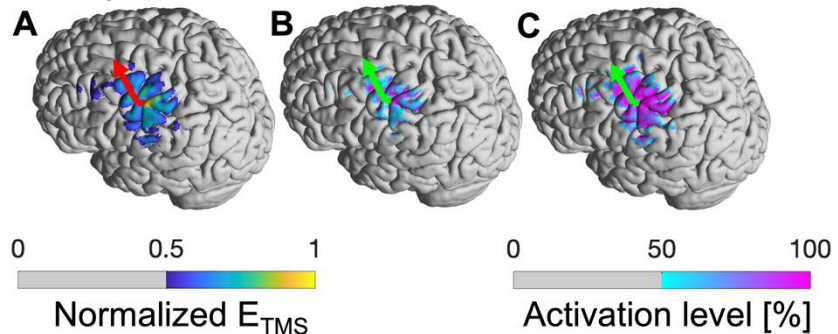


Figure 3. Modelled E-field and activation distributions on the realistic cortical surface. **A)** Normalized E-field strength. The red arrow shows the direction of the strongest E-field. **B)** and **C)** Activation levels at 180 and 220 MA/s, respectively.



5. Discussion

To understand and model the focality of TMS accurately, one must also model the non-linear, electrophysiological properties of the neurons. The presented simulations revealed that the TMS intensity is a vital parameter to adjust both the level of total cortical activation and the focality of TMS.

The suggested high stimulation intensity (Belardinelli et al., 2019) is likely to increase the TEP amplitudes but with the potential risk of compromising focality. An alternative approach, supported by the present simulations, would be to use a relatively low TMS intensity but increase the number of TMS–EEG trials (from which TEPs are computed by averaging). This latter strategy allows one to measure focal cortical TMS responses with good SNR.

Cortical TMS responses depend on the stimulation orientation. The sigmoidal responsiveness of neurons predicts that stimulating closer to the neuronal thresholds results in stronger orientation dependency. Similarly, different motor representation areas should appear more distinct in motor mapping with lower stimulus intensities. However, as motor evoked potentials have relatively high variability (Kiers et al., 1993), a higher number of trials might be required to ensure sufficient reliability.

In the applied model, there were no inter-neuronal connections, and only one neuron type was represented. Furthermore, direct axonal activation in the white matter due to TMS was ignored (Aberra et al., 2020). These simplifications might explain the high threshold intensities compared to the experimental results. However, for the purposes of this work, the qualitative behaviour of the neuronal excitation at different E_{TMS} strengths is more important than the estimated absolute thresholds.

6. Conclusions

The non-linear, electrophysiological response behaviour of neurons to E_{TMS} possibly explains why the effective focality of TMS can be higher than indicated by the E_{TMS} distribution. This implies to favour stimulation intensities close to the neuronal thresholds to maximize the spatial resolution of TMS, and correspondingly to increase the number of stimulus repetitions to maintain a sufficient SNR in TEPs.

Acknowledgments

The work was supported by the Academy of Finland (Grant No. 321631 and 294625), the Jane and Aatos Erkko Foundation, and the European Research Council (ConnectToBrain; No 810377).

References

- Aberra, A. S., Wang, B., Grill, W. M., & Peterchev, A. V. (2020). Simulation of transcranial magnetic stimulation in head model with morphologically-realistic cortical neurons. *Brain Stimulation*, 13(1), pp. 175–189. DOI: 10.1016/j.brs.2019.10.002
- Hines, M. L., and Carnevale N. (2003). *The Handbook of Brain Theory and Neural Networks*. Cambridge, MA: MIT Press. Retrieved from: <https://mitpress.mit.edu/books/handbook-brain-theory-and-neural-networks>
- Kiers, L., Cros, D., Chiappa, K. H., & Fang, J. (1993). Variability of motor potentials evoked by transcranial magnetic stimulation. *Electroencephalography and Clinical Neurophysiology/Evoked Potentials Section*, 89(6), pp. 415–423. DOI: 10.1016/0168-5597(93)90115-6
- Koponen, L. M., Nieminen, J. O., & Ilmoniemi, R. J. (2018). Multi-locus transcranial magnetic stimulation—theory and implementation. *Brain Stimulation*, 11(4), pp. 849–855. DOI: 10.1016/j.brs.2018.03.014
- Nieminen, J. O., Koponen, L. M., & Ilmoniemi, R. J. (2015). Experimental characterization of the electric field distribution induced by TMS devices. *Brain Stimulation*, 8(3), pp. 582–589. DOI: 10.1016/j.brs.2015.01.004
- Belardinelli, P., et al. (2019). Reproducibility in TMS–EEG studies: A call for data sharing, standard procedures and effective experimental control. *Brain Stimulation*, 12(3), pp. 787–790. DOI: 10.1016/j.brs.2019.01.010
- Picht, T., et al. (2011). Preoperative functional mapping for rolandic brain tumor surgery: comparison of navigated transcranial magnetic stimulation to direct cortical stimulation. *Neurosurgery*, 69(3), pp. 581–589. DOI: 10.1227/NEU.0b013e3182181b89
- Ramaswamy, S., et al. (2015). The neocortical microcircuit collaboration portal: a resource for rat somatosensory cortex. *Frontiers in Neural Circuits*, 9, 44. DOI: 10.3389/fncir.2015.00044
- Ravazzani, P., Ruohonen, J., Grandori, F., & Tognola, G. (1996). Magnetic stimulation of the nervous system: induced electric field in unbounded, semi-infinite, spherical, and cylindrical media. *Annals of Biomedical Engineering*, 24(5), pp. 606–616. DOI: 10.1007/BF02684229
- Thielscher, A., Antunes, A., & Saturnino, G. B. (2015). Field modeling for transcranial magnetic stimulation: a useful tool to understand the physiological effects of TMS?. In *2015 37th annual international conference of the IEEE Engineering in Medicine and Biology Society (EMBC)* (pp. 222–225). IEEE. DOI: 10.1109/EMBC.2015.7318340